Elementary Peptide Motifs in the Gas Phase: FTIR Aggregation Study of Formamide, Acetamide, *N*-Methylformamide, and *N*-Methylacetamide

Merwe Albrecht, Corey A. Rice,† and Martin A. Suhm*

Institut für Physikalische Chemie, Universität Göttingen, Tammannstrasse 6, 37077 Göttingen, Germany

Received: May 6, 2008; Revised Manuscript Received: June 10, 2008

Cold, isolated peptide model compounds and their aggregates are generated in pulsed supersonic jet expansions and detected by FTIR spectroscopy in the amide-A region, complemented by amide-I spectra. The most stable, symmetric dimer of formamide is unambiguously assigned in the gas phase for the first time, also by comparison to the analogous acetamide dimer. Efficient quenching of a hot-state Fermi resonance by cooling of the dimers is invoked. As the preferred relative orientation of the C═O and N−H groups in N-methylated formamide and acetamide is trans, these compounds show a fundamentally different dimerization pattern. Their most stable dimers, which would be analogous to those of formamide and acetamide, remain undetected as a consequence of kinetic control in the jet. Accurate benchmark quantities for multidimensional vibrational treatments of these peptide models are derived, and the influence of methyl groups on the N−H stretching dynamics is discussed.

1. Introduction

The peptide bond is among the most important binding motifs in biochemistry. It links amino acids together, provides rigidity to the protein backbone, and contains the two essential docking sites for hydrogen-bond-mediated protein folding and protein aggregation, namely, the C═O acceptor and the N−H donor unit (Figure 1). Via the peptide bond and its zwitterionic resonance structures these two functional groups are intimately linked together in an antiparallel (trans) fashion, offering pathways for cooperativity and anticooperativity[1–4] whenever they undergo hydrogen bonding. The infrared C═O (amide-I) and N−H (amide-A) chromophores thus provide sensitive and extensively used probes into the structure of peptides.[5,6] The N−H chromophore has been argued to exhibit a high degree of adiabatic separability,[7] which makes it a useful sensor for hydrogen-bond interactions in peptides. In weak hydrogen-bond situations[8] it indeed correlates nicely with acceptor strength. On the other hand, N−H bonds in strong hydrogen-bond environments can develop a more complex vibrational dynamics.[9,10] If the two IR chromophore groups are parallel (cis) to each other (Figure 1), they represent a major intermolecular binding motif for DNA.[11]

Most experimental studies refer to condensed phases, the natural environment of proteins and nucleic acids. However, important spectroscopic insights have also been gained by bringing small peptides and DNA fragments into the gas phase. This is usually done at low temperatures, where conformations can be frozen and primary steps of aggregation can be investigated.[12] In particular, the amide-A region profits from supersonic jet cooling because its sensitivity to hydrogen bonding leads to heterogeneously broadened bands in the liquid phase. Remarkably, there remain many open questions for even the simplest peptide and DNA building blocks in the gas phase. The reason is that the simplest model compounds lack a suitable UV chromophore for sensitive double-resonance detection of the vibrational spectrum. Traditional gas-phase data[13,14] suffer from thermal broadening and shifts. In addition, the gas-phase concentration of dimers or larger clusters at thermal equilibrium is usually negligible.

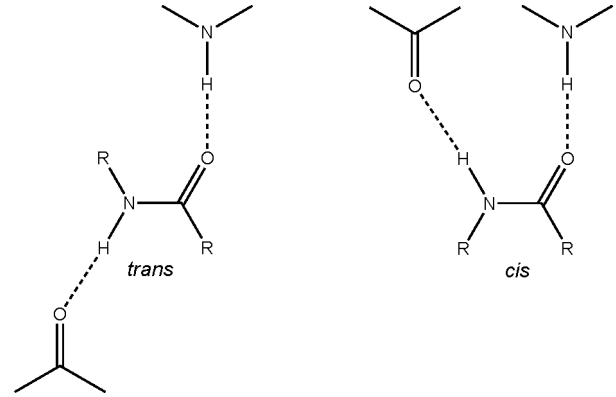

Figure 1. Different arrangements and hydrogen-bond options of the N−H donor and C═O acceptor in the peptide bond and adopted nomenclature for trans and cis N-methylated amides.

This contribution presents and discusses the first direct absorption infrared cluster spectra of formamide and three of its C- and N-methylated derivatives in vacuum isolation at low temperatures. The experimental reference data are expected to provide important benchmark information for theoretical approaches to these model systems,[15] which are indeed numerous and range from harmonic calculations[2,4,16–26] over classical molecular dynamics on DFT surfaces[26–28] to multidimensional variational treatments.[32–34] Furthermore, the spectra of these elementary amides may be compared to those of more complex amides[32–34] and model peptides[12,35] with direct biological relevance.

Formamide, the simplest molecule with a peptide bond, is planar[36] or quasi-planar.[7,37] Its dimer is an important member of testing sets for noncovalent interaction energies.[38,39] The next member in the homologous series, acetamide, may have a

* To whom correspondence should be addressed. E-mail: msuhm@gwdg.de.
† Current address: Department of Chemistry, University of Basel, Klingelbergstrasse 80, CH 4056 Basel.

10.1021/jp8039912 CCC: $40.75
Published on Web 07/30/2008

slightly pyramidal NH_2 equilibrium structure and features a very floppy methyl rotator, but for our purposes, one can treat it as a single conformation.[36] By methylating one of the amide N−H bonds, conformational isomerism around the peptide bond is introduced. For consistency purposes within this paper, we denote the resulting *N*-methylamides as cis (trans) whenever the C═O group and the remaining N−H group are cis (trans) to each other (Figure 1). Note that this convention is not always adopted.[40–43] The trans form is significantly more stable in singly methylated formamide and acetamide. Therefore and also because the barrier to isomerization around the anisotropic peptide bond is rather high, we do not expect to observe clusters of the cis form in our experiments, even if they are significantly more stable. *N*-Methylformamide and, in particular, *N*-methylacetamide have been studied in detail due to their model function in peptide dynamics.[30,44]

After introducing the spectroscopic tools in the next section, the results for the four amides, ordered by increasing complexity, are presented and discussed in section 3. The focus is on the amide-A or N−H stretching region with some additional information presented for the amide-I region. A discussion of methylation and argon matrix isolation trends is followed by the summary in section 4.

2. Methods

The vapor pressure of the investigated amides is rather small at room temperature. Therefore, two different kinds of pulsed supersonic jet expansions[45,46] were employed to generate cold clusters. A sensitive room-temperature 600 mm slit jet (filet jet[47]) was used to probe formamide and *N*-methylacetamide monomers and dimers close to the detection limit. A heated, pulsed, 10 mm long and 0.5 mm wide slit nozzle (popcorn jet)[48] was employed for the study of clusters of all four compounds. The spectrum of *N*-methylfomamide in Figure 7 was obtained using a variant of the popcorn nozzle with two parallel slits of 10 × 0.5 mm^2 in a distance of 10 mm, which were probed perpendicular to the slit direction. It offers enhanced absorption signals. The sample temperatures were usually chosen such that the vapor pressure was on the order of 1 mbar or less. Descriptions of the experimental setups are found elsewhere.[47,49] In short, 0.1−0.3 s gas pulses emerging from the nozzles were synchronized to Fourier transform infrared (FTIR) scans (Bruker IFS 66v or Equinox 55), and the signal was detected by an InSb or HgCdTe detector after optical filtering of unwanted spectral ranges. Maximum overlap between the jet zone and the IR beam is achieved by KBr or CaF_2 lenses, which may be heated in the popcorn-jet setup. In the heated nozzle setup double-sided interferograms were recorded and provided two spectra per scan. Because the gas pulses (He with a trace of the desired compound) in particular from the long slit nozzle are too intense to keep up a sufficient vacuum, they were diluted in large vacuum chambers before being pumped away using mechanical Roots pumps of moderate size (250−2000 m^3/h). This results in a fairly low duty cycle, but the technique is much more sensitive than continuous jet FTIR setups at moderate resolution as it generates higher peak absorbances. The gas mixture was prepared by flowing the He either through a cooled saturator containing the liquid or solid (long nozzle) or through a heated sample container enclosed between two check valves (short nozzles). The container was filled with molecular sieve, which was previously wetted with the liquid or molten compound. In both cases (filet and popcorn jet) the pickup temperature was lower than the nozzle temperature to prevent saturation of the He with the compound of interest and therefore to support a controlled nonequilibrium aggregation. For the heated nozzle additional spectra recorded in the effusive phase at the end of the gas pulse after closing the He supply help in identifying monomer absorptions. Spurious dispersion-like signals were occasionally generated by particulate matter in the jet plume or on the focusing lenses. They could sometimes be minimized by subtracting spectra from the early phase of a measurement sequence, where they were most pronounced.

It is difficult to quantify the effective rotational and vibrational temperatures in our jet expansion spectra, which represent averages over up to 1 cm^2 of the expansion cross section. Higher resolution studies,[50] rovibrational transitions from water impurities, and the scaling of P/R-branch separations with $\sqrt{T}$ all indicate rotational temperatures between 10 and 30 K. The vibrational temperatures are usually higher, around 200 K, where vibrational hot bands could be observed,[8] but probably varying between at least 50 and 300 K for different types of vibration.

Formamide (Fluka, 99%), acetamide (Fluka, 99%), *N*-methylformamide (Alfa, 99%), and *N*-methylacetamide (Aldrich, 99+%) were used as supplied. Traces of water could usually be removed during the first scans due to its higher volatility.

Harmonic force field calculations at the B3LYP/6-311+G* level were carried out using the Gaussian 03 program suite,[51] scaling N−H stretching wavenumbers uniformly by 0.96 and C═O stretching fundamentals by 0.98. There is a large number of literature data on quantum chemical force fields of the investigated compounds, sometimes including higher levels, to which we selectively refer to in the discussion. However, it was deemed necessary to have a uniform albeit approximate approach for all systems[21] for a systematic comparison of the effects of methyl group substitution on the aggregation. We are aware of the fact that subtle monomer NH_2 planarity and methyl group torsional issues are not dealt with adequately at the B3LYP level. For example, acetamide monomer is predicted to have a planar NH_2 group and a C_s-symmetric methyl group at variance with several higher level results[36,52,53] and also the solid-state structure.[54] For an understanding of the dimerization behavior these issues are of secondary importance and some of them already change with inclusion of zero-point motion. Major dispersion interactions are not expected for these elementary systems with polar hydrogen bonds. For MP2 calculations of amide clusters use of a large basis set is nevertheless important. Accurate quantum chemical and quantum dynamical modeling of the four model compounds remains a challenge for theoreticians, to which this work attempts to contribute on the experimental side, as far as cluster formation is concerned.

3. Results and Discussion

Spectroscopic results for the four amides are presented and discussed in order of increasing complexity, i.e., methylation. The emphasis is on benchmark wavenumber data for previous and future multidimensional modeling approaches and the N−H stretching dynamics. The spectra obtained in this range are summarized in Figure 2. At the end, the influence of methylation and matrix embedding on the vibrational dynamics is analyzed.

3.1. Formamide. Three IR bands can be expected in the N−H stretching spectrum of formamide monomer. The symmetric N−H stretching fundamental is slightly perturbed with its unperturbed band center close to 3440 cm^{-1}.[55] The antisymmetric N−H stretching mode is higher in wavenumber, near 3564 cm^{-1}.[37] In between, at 3530 cm^{-1}, the C═O stretching overtone has been assigned to a significantly weaker band.[37] The anharmonic monomer spectrum has recently been studied using the nonrigid bender formalism.[7]

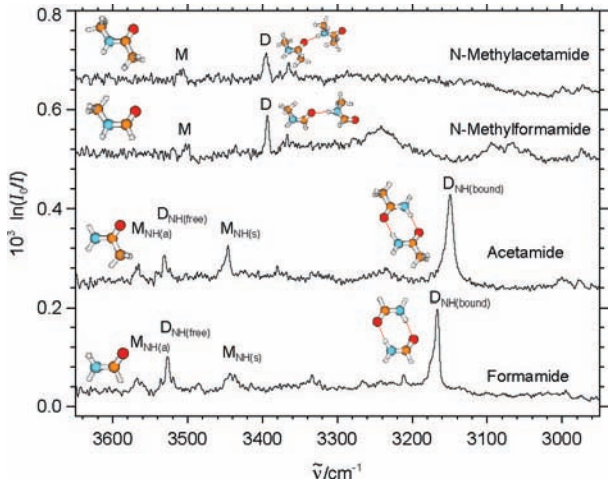

Figure 2. Popcorn-jet spectra of formamide (338 K, 1340 coadded spectra), acetamide (338 K, 606 coadded spectra), *N*-methylformamide (333 K, 600 coadded spectra), and *N*-methylacetamide (323 K, 600 coadded spectra) in the N−H stretching region.

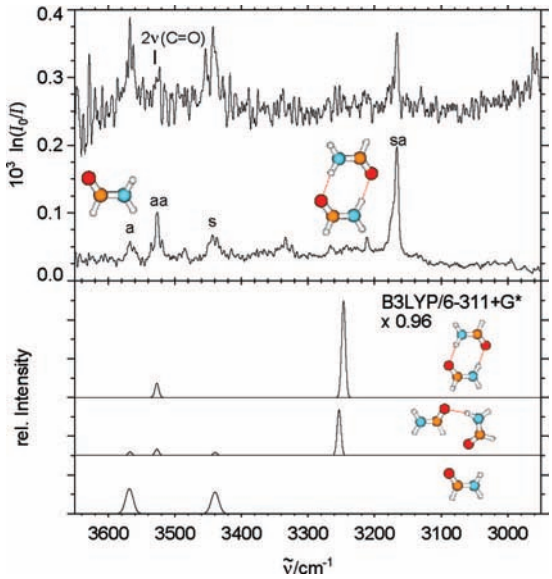

Figure 3. (Top) N−H stretching FTIR spectra of formamide recorded with the filet-jet setup (top, 298 K sample, 450 coadded spectra) and with the popcorn-jet setup (bottom, 338 K sample, 1340 coadded spectra). (Bottom) Calculated wavenumbers for the monomer, the second most stable dimer, and the most stable cyclic dimer at the harmonic B3LYP/6-311+G* level, scaled by 0.96. The calculated dimer intensities are scaled to approximately match with the popcorn-jet spectrum, which contains ∼10% dimer. The expected position[37] of the carbonyl overtone is marked in the top spectrum.

Figure 3 shows two spectra of formamide expansions in He. The upper trace was obtained from a room-temperature expansion through the 600 mm nozzle and the lower trace from an expansion through the 10 mm nozzle with the compound heated to 338 K. All three absorptions expected for the monomer are observed within ±2 cm^{-1} of the room-temperature band centers (see Table 1). However, the center band is significantly stronger in the heated and therefore denser expansion, indicating an additional contribution due to clusters around 3527 cm^{-1}. This correlates with a prominent band near 3167 cm^{-1} in both jet spectra, which also becomes stronger in the heated expansion. Further absorption signals are too weak and unspecific to be identified unambiguously. The comparison of the filet- and popcorn-jet spectra illustrates the advantage of a heatable nozzle. Despite the 60× shorter optical path, monomer absorptions of comparable intensity are obtained in the heated setup. Cluster absorptions are even stronger because higher concentrations of formamide in the carrier gas can be realized.

A straightforward interpretation of the two new bands in the jet spectra is possible in terms of a centrosymmetric dimer (see insert in Figure 3). It is predicted to be particularly stable and expected to have two IR-active and two Raman-active N−H stretching bands. Figure 4 illustrates the evolution from a hypothetical localized N−H stretching mode (loc) via the antisymmetric (a) and symmetric (s) combinations in the monomer to the four modes in the dimer. The latter result from antisymmetric and symmetric combinations of the two monomer modes, denoted by a second 'a' or 's'. The apparent red shift of the 'aa' and 'as' bands relative to the monomer 'a' band is largely a consequence of the localization of the free N−H stretching modes in the dimer. Relative to the average value of the monomer modes 'a' and 's', these dimer modes are even slightly blue shifted. The N−H···O=C hydrogen-bonded modes 'sa' and 'ss' are strongly red shifted relative to the monomer 's' band with the Raman transition (symmetric within the monomer modes and in the two monomers relative to each other, therefore 'ss') falling at the lowest wavenumber. Larger clusters[56] involving the dangling N−H bonds or higher lying dimer isomers[4,26] do not appear to contribute significantly to the spectrum as these would normally affect the hydrogen-bond lengths and thus the N−H stretching spectra quite substantially.[57] However, we should stress that the next most stable dimer[26] (center trace in the bottom part of Figure 3, involving a single N−H···O=C bond along with a weaker C−H···O=C contact) would be difficult to discriminate from the spectrum computed for the global minimum structure at this point and may be present as well.

The only problem with this rather simple interpretation is that it does not fully agree with previous spectroscopic evidence based on matrix isolation and Rydberg electron-transfer infrared spectra. Therefore, an extensive discussion is required to support our straightforward assignment.

We start this discussion by a summary of what is known from quantum chemistry about formamide dimer. Several minima on the potential-energy hypersurface (PES) have been located in a range of studies. By far the most stable structure is the symmetric structure with an inversion center shown in Figure 3 (top part). Its electronic binding energy has been predicted near 62 kJ/mol based on a very extensive ab initio study.[4] The next lowest structure is almost 20 kJ/mol less stable[4] and therefore unlikely to form in significant amounts in our supersonic jet expansions.

Calculated spectra within the double-harmonic B3LYP/6-311+G* approximation (Figure 3, bottom) reveal that the spectrum of the symmetric dimer structure matches the experimental spectrum quite well. Spectra of formamide dimer have been calculated previously at various levels, and we include some of the results[15,18,19,21,23,24,26] in Table 1. In this table the dimer fundamentals are listed relative to their corresponding monomer modes according to Figure 4. Alternatively, one could have tabulated shifts relative to the average of the monomer modes.[58] Quite uniformly, all calculations predict the IR-active free N−H stretching fundamental about 50 cm^{-1} below the antisymmetric monomer stretching mode. Approximate inclusion of anharmonicity[23] reduces the shift to about 30 cm^{-1}. This is in satisfactory agreement with the experimental shift in solution,[18] matrix isolation[59,60] and the supersonic jet,[23] including the present work. For the larger shift of the hydrogen-bonded N−H fundamental the scatter of harmonic predictions is larger

TABLE 1: Harmonic (anharmonic) Formamide Monomer Antisymmetric (a) and Symmetric (s) N−H Stretching Fundamentals and Wavenumber Shifts in the Corresponding Dimer Vibrations for IR (antisymmetric combination of monomer modes, aa and sa) and Raman (Ra, symmetric combination of monomer modes, as and ss) Active Dimer Modes (all in cm^{-1})[a]

method	a	s	as(Ra)	aa(IR)	sa(IR)	ss(Ra)
PW91PW91/6-31+G*[21]	3625	3491	−49	−49	−303	−358
B3LYP/6-311+G(d)	3717 (32)	3583 (28)	−44 (0)	−43 (146)	−201 (1000)	−236 (0)
B3LYP/6-31++G(d,p)[18]	3732 (45)	3587 (36)	−48 (0)	−48 (179)	−246 (1256)	−290 (0)
B3LYP/6-31++G(2d,2p)[23]	3734 (44)	3589 (34)	−52 (0)	−51 (168)	−277 (1337)	−325 (0)
+anharmonic PT[23]	*3527*	*3411*	*−31*	*−31*	*−251*	*−394*
B3LYP/6-311++G(2d,2p)[24]	3726 (45)	3588 (35)	−47 (33?)	−47 (135)	−258 (1279)	−303 (0)
B3LYP/aug'-cc-pvdz[19]	3709 (42)	3564 (34)	−49 (0)	−49 (164)	−283 (1400)	−335 (0)
MP2/6-31G(d,p) [15]				−60	−216	
MP2/cc-pVTZ[26]	3787	3635		−58	−273	
Ar matrix[61]	3555	3430		−37	−300	
Ar matrix[59,60]	3548	3427		−33	−211	
					−232	
Ar matrix[26,96]	3547	3427		−32	−296	
Xe matrix[26]	3537	3411		−38	−253	
CCl_4 solution[18]	3534	3411		−36	−182	
jet RET[23]	3568	3442		−36	−219	
					−259	
jet FTIR (this work)	3564	3440		−37	−273	
gas phase[37,55]	3564	3440				
gas phase[61]	3570	3448				

[a] Calculated IR band strengths in km mol^{-1} are listed in parentheses. Comparison is made between the lowest energy predicted structure and experimental (*anharmonic*) monomer band centers and dimer shifts.

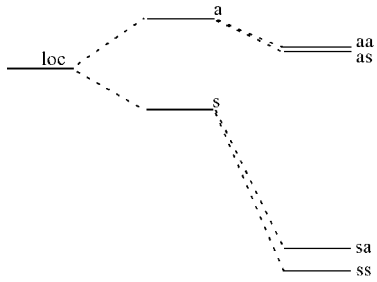

Figure 4. Qualitative evolution of the N−H stretching mode in an NH_2 group from a local mode picture (loc) via the coupled monomer situation (a, s) to the symmetric dimer (aa, as, sa, ss). The first label refers to the relative phase of the two monomer stretching modes and the second label to the relative phase between the two monomers in the dimer.

(200−300 cm^{-1}), but most values are quite close to our experimental anharmonic value of 273 cm^{-1}. Experimental values for embedded formamide dimers are remarkably smaller in some cases (Table 1). For the CCl_4 solution[18] this is not surprising because thermal excitation weakens the hydrogen bonds. Therefore, the assignment to the centrosymmetric dimer in that study is consistent with our observation at low temperature. For the cryogenic matrix value[59,60] it is more unusual as the monomer matrix shifts are only on the order of 15 cm^{-1} [60] in Ar and somewhat larger in Xe[26] (see also section 3.6 below). It is conceivable that similar to solid formamide,[57] interaction of the free N−H groups with Ar and Xe matrix atoms weakens the dimer N−H···O═C hydrogen bonds. The fact that two bands separated by 21 cm^{-1} are observed in some Ar matrix studies also points to important matrix interactions such as site splittings. On the other hand, some Ar matrix data are more consistent with our jet spectra.[26,61] Furthermore, a single band is also listed for other matrices such as CO and N_2.[59] Therefore, the matrix isolation data are not fully consistent among each other but can mostly be reconciled with the jet data.

Finally, the intensity ratio between the bonded and the free N−H dimer stretching vibration is predicted to be between 5 and 10 at the various levels of approximation. This is consistent with our experimental value, which cannot be quantified exactly due to the overlap with the monomer C═O overtone. In summary, the isolated formamide dimer spectrum with a single strongly red-shifted band can be reconciled with most of the previously available embedded spectra considering the possible artifacts which embedding can produce.

Quite surprisingly, the recent supersonic jet spectrum of formamide dimer based on Rydberg electron transfer (RET)[23] contains two red-shifted bands of similar strength reasonably close to some of the Ar matrix positions[59,60] but not to our dominant jet band. In this innovative technique vibrational spectra are recorded by monitoring the electron-capture process as a function of vibrational pre-excitation. The authors postulate that the mutual Raman/IR exclusion rule may be lifted in their experiment such that the Raman-active band of the cyclic dimer is observed as well in the IR. This appears unlikely despite the action spectroscopy character of the RET experiment as the absorption step occurs first. Furthermore, the Raman band is expected at significantly lower wavenumber based on all harmonic predictions, and the anharmonic value is likely to be even lower.[23,62] Currently, the sensitivity of our Raman jet spectrometer[63] is not sufficient to observe the totally symmetric stretching vibration.

We can only speculate why the RET experiment[23] finds two hydrogen-bonded N−H stretching bands, both of which are blue shifted from the single band observed in this work. The RET process may favor a higher-lying, dipolar isomer of formamide dimer despite its low abundance. Our FTIR spectra indeed show some weak absorption features in the range of the RET signals. Alternatively, the high dissociation threshold of the cyclic dimer may distort its action spectrum observed in the RET experiment. In particular, it is conceivable that hot dimers contribute most to the RET spectrum, and there could be a similar hot Fermi resonance scenario as in acetamide, described in the following section.

The carbonyl stretching (or amide-I) band[5,20] was also investigated in the jet-FTIR expansion (Figure 5). However, the separation between monomer and dimer absorptions is not large enough to allow for unambiguous conclusions in this range.

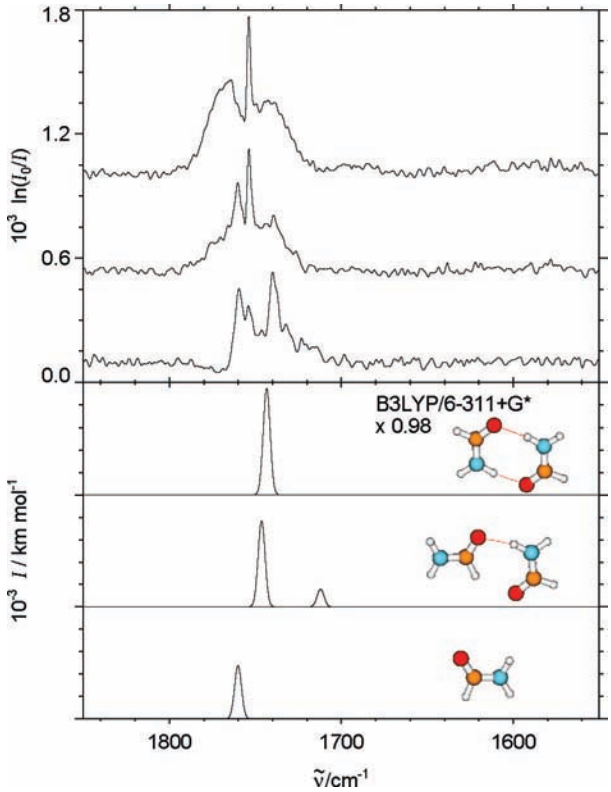

Figure 5. Carbonyl stretching FTIR jet spectrum of formamide (bottom of the top half, 338 K sample, 400 coadded spectra) and effusive gas-phase spectra recorded immediately after the jet expansion (middle and top trace, 400 coadded spectra each). They are compared to the calculated wavenumbers for the monomer, the second most stable dimer, and the most stable cyclic dimer at the B3LYP/6-311+G* level, scaled by 0.98.

TABLE 2: Harmonic Formamide Monomer (M) and Dimer (D) Carbonyl Stretching Vibrations and Wavenumber Shifts between the Monomer and Dimer Bands (in cm^{-1})[a]

method	$\nu_{C=O}$ (M)	$\nu_{C=O}$ (D)	$\Delta\nu_{C=O}$
PW91PW91/6-31+G*[21]	1754	1738	−16
B3LYP/6-311+G(d)	1796 (477)	1779 (947)	−17
B3LYP/6-31++G(d,p)[18]	1797 (459)	1782 (911)	−15
B3LYP/6-311++G(2d,2p)[20]	1781 (442)	1765 (870)	−16
B3LYP/6-311++G(2d,2p)[24]	1783 (440)	1765 (872)	−18
MP2/6-31+G(d)[20]	1795 (443)	1796 (896)	−1
MP2/cc-pVTZ[26]	1811	1802	−9
Ar matrix[61]	1743	1728	−13
	1739		
Ar matrix[26]	1739	1728	−11
Xe matrix[26]	1731	1719	−12
jet FTIR (this work)	1754	1740	−14
gas phase[37,55]	1754		
gas phase[61]	1755		

[a] Comparison is made to experimental (anharmonic) monomer and dimer band centers and the resulting dimer shift. Calculated IR band strengths in km mol^{-1} are listed in parentheses.

Furthermore, it is possible that larger clusters contribute. The dispersion-like feature on the high-wavenumber slope may result from imperfectly compensated formamide deposits on the optics. Nevertheless, a bathochromic dimer shift by about 14 cm^{-1} can be extracted from the dominant spectral features. In Table 2 this shift is compared to calculated values and matrix data. The calculated shift between the carbonyl stretching vibration of the monomer and dimer falls in a range of 15−18 cm^{-1} except for MP2 predictions, which are much smaller. This may be due to basis set deficiencies, like in the related pyrrole carboxaldehyde

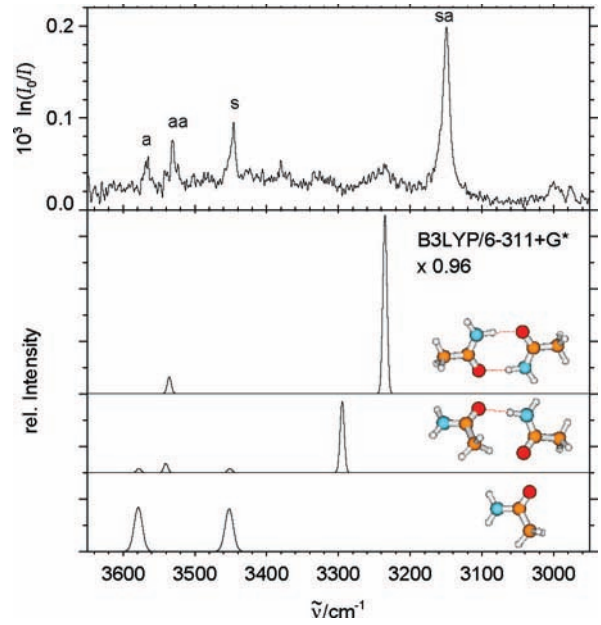

Figure 6. N−H stretching FTIR jet spectrum of acetamide (substance at 338 K, 600 coadded spectra) compared to the calculated wavenumbers for the monomer, the second most stable dimer, and the most stable cyclic dimer at the B3LYP/6-311+G* level, scaled by 0.96. The calculated dimer intensities are divided by 12 to match with the approximate experimental monomer/dimer ratio, implying a dimer fraction of ∼7%.

case.[64] The dimer shifts in matrices[26,61] also agree well with the jet result, although they are comparable to the matrix-induced shift itself.

Apart from the strong bands at 1754 and 1740 cm^{-1} in the jet spectrum, a third prominent band occurs at 1760 cm^{-1}. This band initially survives the collapse of the jet expansion (shown in the upper two traces of Figure 5). It is therefore likely that it has a monomer origin. Indeed, no blue-shifted dimer band is expected from the calculations. Interestingly, there is a similar blue-shifted and unassigned band in the recent matrix spectra (ref 26 Figure 4). It remains unclear whether both bands have the same origin as the matrix band depends on the embedding matrix and may also be due to a site splitting.

Overall, the jet spectra are consistent with a dominance of symmetric formamide dimers, but contributions by a less stable dimer with a single N−H···O=C hydrogen bond cannot be ruled out at this stage. In such a situation it is meaningful to switch to the homologous compound acetamide.

3.2. Acetamide. Figure 6 shows a popcorn-jet spectrum of acetamide recorded under similar conditions as that of formamide (Figure 3). The appearance of the spectrum is also quite similar with two strong monomer bands ('a' and 's') and two IR-active dimer bands ('aa' and 'sa'). Weaker bands between 'aa' and 'sa' may be due to larger clusters or a dimer Fermi resonance pattern, like in the related acetic acid case.[65] The monomer band positions (Table 3) may be compared to earlier gas-phase spectra recorded at 453−483 K.[14] While the value for the symmetric N−H stretching mode agrees, the antisymmetric one was observed at a somewhat lower wavenumber in the hot gas phase than in the jet (Table 3).

Acetamide has been extensively studied by matrix isolation techniques.[66–68] The band for the antisymmetric N−H stretching fundamental was found at 3552 cm^{-1} and the symmetric N−H stretching fundamental at 3432 cm^{-1} in an argon matrix.[66,67] The monomer matrix red shift is 12−16 cm^{-1}, similar to that

TABLE 3: Harmonic Acetamide Monomer Antisymmetric (a) and Symmetric (s) N−H Stretching Fundamentals and Wavenumber Shifts in the Corresponding Dimer Vibrations for IR (antisymmetric combination of monomer modes, aa and sa) and Raman (symmetric combination of monomer modes, as and ss) Active Dimer Modes (all in cm^{-1})[a]

method	a	s	as(Ra)	aa(IR)	sa(IR)	ss(Ra)
B3LYP/6-311+G(d)	3728 (28)	3596 (27)	−45 (0)	−45 (129)	−226 (1365)	−262 (0)
MP2/cc-pVTZ[53]	3797	3653				
Ar matrix[66,67]	3552	3432				
Ar matrix[68]	3557	3436		−42	−296	
$CHCl_3$ solution[70]	3533	3415		−32	−225	
$CHCl_3$ solution[58]	3535	3417		−35	−227	
phenylacetamide[32]	3556	3438		−56	−303	
jet FTIR (this work)	3568	3448		−37	−299	
gas phase[14]	3550	3450				
GC-IR[73]	3570	3450				

[a] Comparison is made between the lowest-energy predicted structure and experimental (anharmonic) monomer band centers and dimer shifts. Calculated IR band strengths in km mol^{-1} are listed in parentheses.

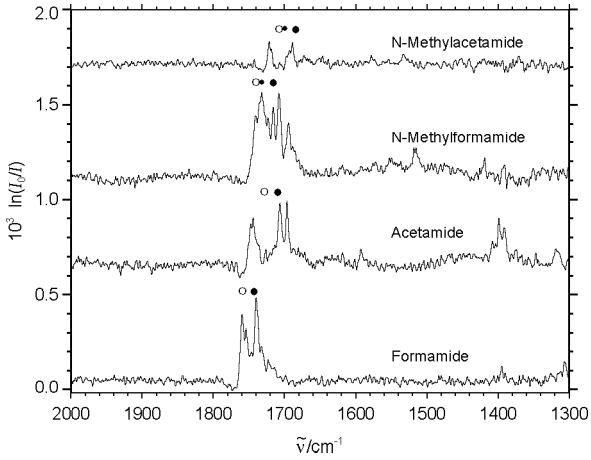

Figure 7. Popcorn-jet spectra of formamide (338 K, 500 coadded spectra), acetamide (338 K, 710 coadded spectra), *N*-methylformamide (323 K, 700 coadded spectra, double slit nozzle), and *N*-methylacetamide (323 K, 600 coadded spectra) in the C═O stretching region. The calculated wavenumbers (scaled by 0.98) of the monomers are symbolized with ○ and the ones of the dimers with ●. For the N-methylated amides the less intense dimer band is symbolized with a smaller ●.

of formamide. Our B3LYP calculations predict the a/s splitting and the intensity pattern reasonably well, as was the case for formamide.

The shifts of the dimer bands relative to the corresponding monomer transitions compare well with those observed in an earlier matrix isolation study[68] (Table 3), although the latter suffers somewhat from site splittings in the monomer range. The matrix study[68] assigns the dimer bands to a structure with a single hydrogen bond. As the B3LYP simulations in Figure 6 show, an assignment to the cyclic dimer (upper trace) fits better and is more plausible in view of its higher stability. The singly bound structure (center trace) now involves a methyl C−H instead of an amide C−H and is about 20 kJ/mol higher in energy than the cyclic dimer at the B3LYP level. Furthermore, the predicted formamide coincidence of the most red-shifted bands of the two lowest dimer structures is removed in acetamide. Presumably the methyl C−H is an inferior secondary hydrogen-bond donor to the amide C−H. This is reminiscent of the acetic acid case,[69] but the spectral separation is less pronounced. Since the experimental spectrum still shows a single dominant low-wavenumber N−H stretching band, the ambiguity concerning the isomer assignment is removed. We can now safely assign the dominant features of the formamide and acetamide jet spectra to the antisymmetric hydrogen-bonded N−H stretching mode in a centrosymmetric dimer.

Independent evidence for the cyclic dimer structure comes from a UV/IR double-resonance study of the phenyl derivative of acetamide[32] (phenylacetamide, see Table 3). Its band positions are very similar to those observed here for the unsubstituted monomer and dimer, which are more accessible to high-level quantum chemistry calculations. In acetamide, we also find weak evidence for secondary dimer bands, which have been attributed to combinations of lower wavenumber fundamentals.[32]

There is earlier evidence for acetamide aggregates in $CHCl_3$ solution.[58,70] The shift between the antisymmetric N−H stretching vibration of the monomer and the 'aa' vibration of the dimer is similar to the jet value, whereas the shift between the symmetric N−H stretching vibration of the monomer and the 'sa' vibration of the dimer is underestimated in comparison with the jet value. This is again a consequence of the thermal weakening of the hydrogen bond at the solvent temperature. The 'sa' band in solution is split, which has been attributed to a Fermi resonance with the first overtone of the bending mode δ_{NH_2}.[58] Such a resonance possibility is also suggested by our harmonic B3LYP/6-311+G* calculations of the cyclic acetamide dimer, where the two states lie quite close together in energy. However, anharmonic contributions are sizable and may act in different directions for the resonance partners. A close resonance in the jet can be ruled out due to the relatively narrow 'sa' band profile. It is remarkable that a nearly perfect Fermi resonance in chloroform solution with a coupling matrix element of about 65 cm^{-1} is completely quenched by jet cooling. The common zero-order band position of ∼3270 cm^{-1} of the two states in chloroform transforms into a stretching transition in a cold and thus more strongly bound complex at 3150 cm^{-1} (see also Table 1 for the related behavior in formamide) and a stiffened bending overtone transition above 3300 cm^{-1}. It would be interesting to study this Fermi resonance quenching as a function of cooling.

The solid state of acetamide[71,72] consists of a hydrogen-bonded network of interconnected rings of six monomer units, where every monomer donates and accepts two hydrogen bonds. The donors are the two hydrogen atoms of the NH_2 group, and the acceptor is the carbonyl oxygen. The hydrogen-bond distances are 2.91−2.95 Å.[71] Calculation for the cyclic dimer predicts a similar hydrogen-bond length of 2.91 Å (B3LYP/6-311+G*). The solid-state N−H bands appear at 3160 and 3330 cm^{-1},[14] reflecting coupled vibrations or the Fermi resonance discussed above. In any case, the absence of the 3330 cm^{-1} band excludes the presence of large solid-like clusters in our jet expansion.

The amide-I or carbonyl stretching region of acetamide is not as widely studied as the amide-A or N−H stretching region. Our theoretical and experimental results for the carbonyl stretching vibration are compared to the literature values in Table 4. The pioneering gas-phase value[14] for the $\nu_{C=O}$ mode (1733 cm^{-1}) differs somewhat from the jet monomer band maximum at 1746 cm^{-1}, probably due to thermal excitation. The agreement for the δ_{NH_2} bending mode at 1593 cm^{-1} (amide-II band) is better. Gas-chromatographic IR data (GC-IR) reported in the NIST database[73] show even better agreement in their graphically

TABLE 4: Harmonic Acetamide Monomer (M) and Dimer (D) $\nu_{C=O}$ Carbonyl Stretching Vibrations and δ_{NH_2} Bending Vibrations as well as Wavenumber Shifts between the Monomer and Dimer Bands (all in cm^{-1})[a]

method	$\nu_{C=O}$ (M)	$\nu_{C=O}$(D)	$\Delta\nu_{C=O}$	δ_{NH_2} (M)	δ_{NH_2} (D)	$\Delta\delta_{NH_2}$
B3LYP/6-311+G(d)	1765 (425)	1745 (876)	−20	1655 (89)	1681 (74)	26
B3LYP/6-311++G**[53]	1762			1622		
B3LYP/6-311++G(2d,2p)[20]	1752 (394)			1625 (92)		
MP2/6-31+G*[20]	1780 (354)			1663 (94)		
MP2/cc-pVTZ[53]	1805			1641		
Ar matrix[68]	1728	1694	−34	1586	1620	34
Ar matrix[66]	1727			1585		
$CHCl_3$ solution[70]	1700	1678	−22		1595	
jet FTIR (this work)	1746	1706	−40	1593		
gas phase[14]	1733			1600		
GC-IR[73]	1742			1590		

[a] Comparison is made to experimental (anharmonic) monomer and dimer band centers and dimer shifts. IR band strengths in km mol^{-1} are listed in parentheses.

estimated band centers (1742 and 1590 cm^{-1}). In Ar matrices and solution, the monomer band positions are bathochromically shifted.

The strongest dimer feature in the jet appears 40 cm^{-1} below the monomer C═O stretching band (see Figure 7). In the matrix and solution the shift is smaller. This is also the case for the harmonic B3LYP prediction. Nevertheless, the dimer assignment is unambiguous as concentration dependency studies show. A further red-shifted band attributed to larger clusters due to its stronger concentration dependence appears in the jet at 1696 cm^{-1}. The dimer δ_{NH_2} bending mode is too weak and broad to be located unambiguously in the jet spectrum, but it has been assigned by matrix isolation and in solution. Its blue shift relative to the monomer is described well by the B3LYP calculations.

3.3. N-Methylformamide. While the homologues formamide and acetamide are seen to be very similar in their aggregation signature, *N*-methylformamide introduces a new aspect. Methylation of one of the N−H bonds has two important consequences. Only a single chromophore remains in the N−H stretching range, but two well-separated monomer conformations become possible. The cis/trans nomenclature adopted for them in this work is described in Figure 1. The cis form should show a similar aggregation behavior to formamide and acetamide, whereas the trans form and also mixtures of the two can only dimerize via a single N−H···O═C bond. The interesting twist is that the trans form is more stable in the monomer, whereas the cis form is expected to be more stable in the dimer as it allows for two strong hydrogen bonds. This leads to a noteworthy aspect of kinetic control in the jet experiment because the barrier between the two monomer conformations is very high as a consequence of the partial double-bond character of the amide bond.

The situation is illustrated schematically in Figure 8. At the zero-point energy corrected B3LYP/6-311+G* level the cis dimer is 28 kJ/mol more stable than the trans dimer relative to the corresponding fragments. Relative to two trans monomers, the energy difference is still 20 kJ/mol. As the monomer isomerization barrier is about 89 kJ/mol and the monomer energy difference amounts to about 5−8 kJ/mol[25,74] (4 kJ/mol at the B3LYP/6-311+G* level), there will be neither a substantial cis monomer population before the expansion nor a significant interconversion during the expansion, unless there is a much lower barrier isomerization pathway for the dimers or the nozzle is heated to high temperatures. The former is unlikely, whereas the latter can in principle be achieved. At room temperature the relative cis monomer abundance has been estimated to be around 0.05−0.18.[25,75−77] The most recent value is 0.05 in the gas phase (with an enthalpy difference of 7−8 kJ/mol) but about twice as high in solution and in the neat liquid.[25] This means that rather high temperatures will be needed to produce significant amounts of cis-cis collisions.

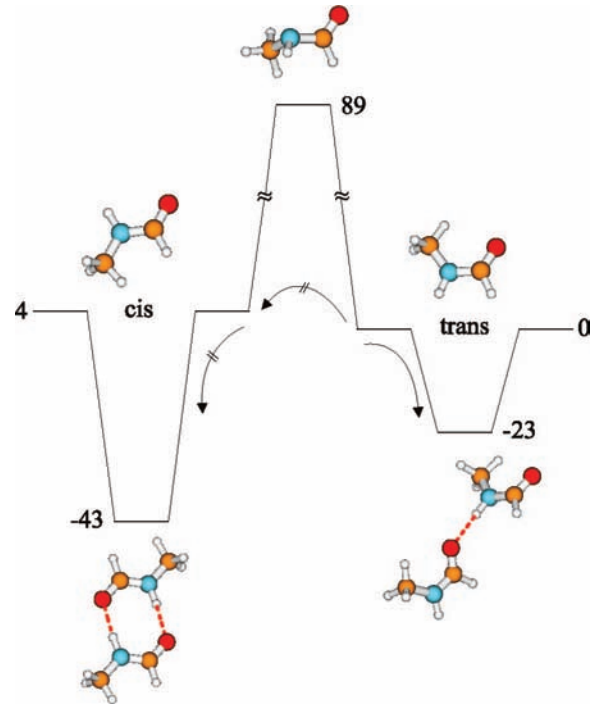

Figure 8. Schematic energy diagram for dimerization and isomerization of *N*-methylformamide (numbers in kJ/mol from B3LYP/6-311+G* calculations including zero-point energy corrections). In the jet expansion, isomerization from the trans to the cis conformation does not occur and the cis dimer is not detected due to the low cis monomer population.

There have been numerous spectroscopic studies of *N*-methylformamide because it can be considered as one of the simplest model systems for protein vibrational dynamics. A recent summary is given in ref 25. In the hot gas phase the N−H stretching mode was observed as a broad, structured band near 3480 cm^{-1} [13,78] whose conformational assignment was corrected later.[76,77] Our popcorn-jet spectra (Figure 9) indeed show a monomer band at 3501 cm^{-1} (see Table 5). The difference may be attributed to thermal broadening and limited resolution in the earlier work.[13] N_2 and Ar matrix isolation values[25,74] are also in reasonable agreement (see Table 5) considering expected matrix shifts. The matrix spectra reveal the cis isomer, which absorbs at 37−38 cm^{-1} lower wavenumber[25] in the N−H stretching range and can be enhanced by

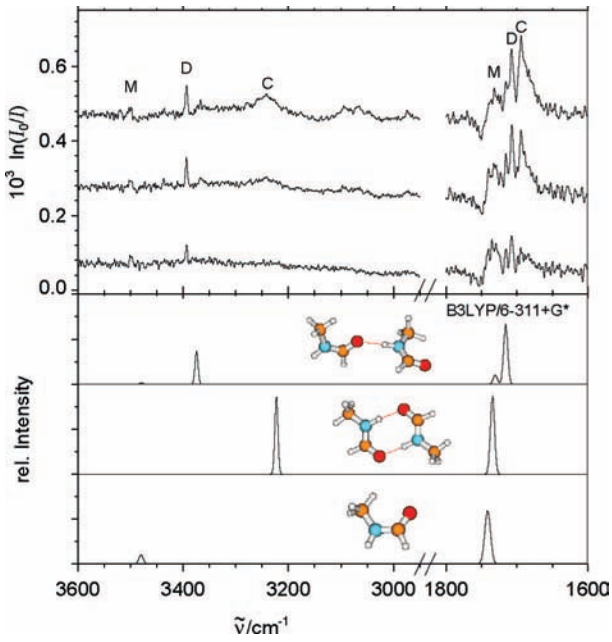

Figure 9. N−H and C═O stretching FTIR jet spectra of *N*-methylformamide at 313 (bottom, 600 coadded spectra each), 323 (middle), and 333 K (top) in comparison to calculated wavenumbers for the trans monomer, the cis-cis cyclic dimer, and the trans-trans dimer. The calculated N−H stretching wavenumbers are scaled by 0.96 and the carbonyl stretching wavenumbers by 0.98. The calculated dimer intensities are divided by 2, and the intensity of the N−H stretching vibration of the monomer is multiplied with 4 to be visible in the plot.

TABLE 5: Harmonic (anharmonic) *N*-Methylformamide and *N*-Methylacetamide Monomer N−H Stretching Vibrations ν_{N-H} (M) as well as the Wavenumber Shifts between the Monomer and Dimer Bands ($\Delta\nu_{N-H}$) (all in cm^{-1})[a]

	N-methylformamide		*N*-methylacetamide	
method	ν_{N-H} (M)	$\Delta\nu_{N-H}$	ν_{N-H} (M)	$\Delta\nu_{N-H}$
HF/6-31+G*[79]	3895 (50)		3866 (43)	
CPMD[28]			3344	
CC-VSCF[29]			*3523*	
CC-VSCF, MP2/DZP[30]			*3542*	
B3LYP/6-31G*[16]			3638 (16)	−52 (369)
B3LYP/6-31+G*[22]			3643 (23)	−106 (504)
B3LYP/6-311+G*	3625 (17)	−110 (491)	3652 (19)	−114 (456)
PW91PW91/6-31+G*[21]			3543	−171
MP2/aug-cc-pVTZ[31]			3703	
+ *mode coupling*[31]			*3531*	
N_2 matrix[74]	3490		3498	
Ar matrix[25]	3493	−81		
CCl_4 solution[22]			3475	−84
jet FTIR (this work)	3501	−107	3510	−115
gas phase[13]	3480			
gas phase[78]	3504		3501	
	3494		3489	
	3482			
	3471			
GC-IR[73]	3480		3490	

[a] Comparison is made to experimental (*anharmonic*) monomer band centers and dimer shifts. IR band strengths in km mol^{-1} are listed in parentheses.

heating the deposition nozzle up to 770 K.[74] No corresponding band could be found in the jet spectrum up to a nozzle temperature of 443 K, confirming the low abundance of the metastable conformation in the jet expansion.

Similar to the case of acetamide, the detailed trans monomer structure of *N*-methylformamide is still under debate,[41] in particular with respect to the conformation of the methyl group (staggered vs eclipsed), which has a very low rotation barrier.[40–42] This also refers to quantum-chemical studies[42,79,80] but is not critical in the present context.

There are several possibilities for formation of *N*-methylformamide dimers consisting of two trans monomers taking the orientation of the two monomers into account. The most stable dimers were found to be T-shaped, not planar.[25] According to our DFT calculations these trans dimers are very easy to distinguish from formamide-like cis dimers. At the B3LYP/6-311+G* level, the shift for the hydrogen-bonded N−H stretching vibration in the trans-trans dimer is predicted to be −110 cm^{-1}, whereas the shift for the cis-cis dimer is predicted to be twice as large (−239 cm^{-1} relative to the cis monomer). On a per hydrogen-bond basis, the hydrogen bond in the *N*-methylformamide dimer formed of two trans monomers is about as strong as one hydrogen bond in the cyclic formamide dimer. The reason for the reduced shift in the trans dimer could reside in the coupling of the two oscillators,[81] in reduced charge shifts,[3] or in a structural effect. A detailed investigation of this effect is beyond the scope of this contribution, but a few pieces of evidence shall be presented. A T-shaped formamide dimer is predicted to exhibit even weaker red shifts because of the coupling of the two N−H oscillators (−50 and −82 cm^{-1}), but their cumulative red shift is comparable to that of the trans *N*-methylformamide dimer. The central N−H in a chain-like trans *N*-methylformamide trimer has a shift of −162 cm^{-1} at the B3LYP level, i.e., significantly larger than in the trans dimer but still less than in the cis dimer.

On the basis of these predictions, the interpretation of the jet N−H stretching spectrum at low concentration (Figure 9, bottom experimental trace) is straightforward. A sharp dimer band (D) red shifted by 107 cm^{-1} from the monomer band (M) is observed and must be attributed to a trans dimer (Table 5). In an Ar matrix[25] a significantly smaller shift was obtained. Only at higher concentration (obtained by a higher sample temperature) does a broad, more strongly red-shifted band (C) appear in the jet spectrum along with some very weak absorptions in between. While it would fit with the spectral prediction of the cis dimer, it is more likely due to larger chain or ring clusters. Further red-shifted peaks may be due to Fermi resonance partners in these larger clusters.

The C═O stretching range is also included in Figure 9 and indicates further complexity. The negative, dispersion-like features on the blue wing of the monomer may be attributed to scattering effects from *N*-methylformamide nano- and microparticles formed in the expansion or deposited on the focusing lenses of the vacuum chamber. They are most pronounced for narrow transitions with a strong monomer transition dipole moment, such as the C═O stretching fundamental. Moderate heating of the focusing lenses in the sample chamber helps in reducing this artifact (see also Figure 7). However, the D and C bands can be correlated between the N−H and C═O spectra and suggest a bathochromic trans dimer shift of ∼24 cm^{-1} for the strongest dimer C═O band, which may be compared to the B3LYP prediction of 26 cm^{-1}. The accuracy of the experimental shift is limited by the structured monomer band rather than by the relatively sharp dimer transition. The monomer C═O band has also been observed in matrix isolation (Table 6), featuring typical matrix shifts. However, no dimer bands have been tabulated in this range, only allowing for an approximate graphical estimate.

TABLE 6: Harmonic (anharmonic) *N*-Methylformamide and *N*-Methylacetamide Monomer (M) Carbonyl Stretching Vibrations and Wavenumber Shifts between the Monomer and Dimer Bands[a]

	N-methylformamide			*N*-methylacetamide		
method	$\nu_{C=O}$ (M)	$\Delta\nu_{C=O}$	$\Delta\nu_{C=O}$	$\nu_{C=O}$ (M)	$\Delta\nu_{C=O}$	$\Delta\nu_{C=O}$
B3LYP/6-311+G(d)	1777 (390)	−11 (140)	−26 (871)	1744 (300)	−11 (102)	−25 (696)
B3LYP/6-311++G(2d,2p)[20,21]	1763 (365)			1739 (285)	−17 (31)	−26 (720)
B3LYP/6-31G*[16]				1792 (240)	−7 (8)	−21 (637)
PW91PW91/6-31+G*[21]				1706	−14	−26
MP2/6-31+G*[20,21]	1770 (362)			1753 (399)	−3 (15)	−12 (784)
CPMD [28]				1609		
CC-VSCF [29]				*1751*		
CC-VSCF, MP2/DZP[30]				*1749*		
MP2/aug-cc-pVTZ[31]				1749		
+ mode coupling[31]				*1727*		
Ar matrix[25,6]	1725		∼−20	1708		−22
N_2 matrix[6]				1706		−25
N_2 matrix[74]	1721			1707		
jet FTIR (this work)	1732		−24	1722		−32
gas phase[97]	1727			1718		
gas phase[13,17]	1724			1723		
gas phase[78]	1759			1731		
	1733			1713		
	1726					
GC-IR[73]	1735			1720		

[a] Comparison is made to experimental (*anharmonic*) monomer and dimer band centers and dimer shifts. Values are given in cm^{-1}. IR band strengths in km mol^{-1} are listed in parentheses.

We close this section with a brief survey over the hydrogen-bond topology obtained from liquid-phase *N*-methylformamide studies. Although the cis dimer is significantly more stable than the trans dimer, the monomer trans preference survives in the condensed phase.[82] More bulky N-substituents than methyl groups can shift the equilibrium somewhat.[83] The reason for the persistent trans propensity is that bulk phases can avoid dangling N−H bonds by extensive chain and network formation. The detailed hydrogen-bond topology in liquid *N*-methylformamide is still under debate.[25] Hexameric rings and linear tetramers have been postulated to be the dominant species.[84] The transition between chains and rings was located between tetramers and pentamers.[84] At higher temperatures mainly linear trimers and dimers are postulated in the liquid, but the underlying quantum cluster equilibrium may be generally biased toward cyclic structures, and the cis monomer was not included in the study. Shin et al. deduced that the trans form prefers to build long chains and that the cis form can serve as a chain blocker (as it interacts more strongly with a trans structure than a trans structure itself) and has a tendency to form strongly bound dimers.[25]

3.4. N-Methylacetamide. *N*-Methylacetamide is particularly well studied because its methyl substitution pattern makes it a more complete but still simple peptide fragment, which can serve as a model for a range of dynamical studies.[85] The hot gas phase of *N*-methylacetamide was investigated by Jones,[78] and the band position of the N−H stretching vibration was found to be similar to that of *N*-methylformamide with the center of gravity at slightly higher wavenumber (see Table 5). The weak monomer band in the jet spectrum (Figure 2) confirms this, provides a more accurate band center, and suggests the presence of a single monomer conformation in the expansion. These findings are in line with matrix isolation results,[74] where a matrix shift of about 10 cm^{-1} has to be taken into account. The *N*-methylacetamide monomer indeed shows an even more pronounced preference for a trans orientation of the C═O and N−H groups than *N*-methylformamide.[83] The calculated energy difference between trans and cis *N*-methylacetamide is about 10 kJ/mol,[86] confirmed by our B3LYP/6-311+G* calculations. The transition barrier is sizable (about 76 kJ/mol[87]), making an interconversion unlikely in jet expansions.

The structure of trans *N*-methylacetamide has been calculated at various levels of theory and involves subtle isomerism over low barriers concerning the two methyl group conformations.[1,43] Therefore, the conformation calculated at the B3LYP/6-311+G* level may not correspond to the global minimum, but the differences between eclipsed and staggered structures are hardly relevant for the hydrogen-bond effects investigated here.

Other than acetamide and *N*-methylformamide, *N*-methylacetamide has been repeatedly addressed by multidimensional anharmonic approaches to the vibrational dynamics,[29–31] rendering our cold jet data (3510 cm^{-1} for the NH stretching fundamental) particularly relevant also for the monomer. Gregurick et al.[29] obtained an ab initio harmonic wavenumber of 3751 cm^{-1} and an anharmonic value of 3523 cm^{-1} using a correlation-corrected vibrational SCF approach at the MP2/DZP level. Bounouar et al.[30] calculated an ab initio harmonic wavenumber of 3752 cm^{-1} and an anharmonic value of 3542 cm^{-1} using a very similar approach. The multidimensional MULTIMODE calculations by Kaledin et al.[31] involving selected three-mode couplings at the MP2/aug'-cc-pVTZ level result in a harmonic value for the N−H stretching vibration of 3703 cm^{-1} and a 3D anharmonic value of 3531 cm^{-1}. All calculated values were originally compared to the experimental matrix value of 3498 cm^{-1} [74] because the gas-phase band[78] is very broad and no other accurate experimental value for the N−H stretching vibration of *N*-methylacetamide was available. The present value of 3510 cm^{-1} extracted from our jet spectra provides a more reliable reference. It should be a better value for any test of the theoretical methods, although the matrix shift is relatively small for this particular band and system. Apart from residual errors in the multidimensional treatments, the results indicate that the harmonic MP2 values may be somewhat too high or else the anharmonicity too small. The DFT-based Car−Parrinello molecular dynamics simulations by Gaigeot et al.[28] of the gas phase of *N*-methylacetamide monomer at 20 K predict 3344 cm^{-1} for the N−H stretching vibration band. This value differs substantially from the experimental value, in

particular considering that this classical procedure provides essentially a harmonic value for temperatures below several 1000 K.

Turning now to dimers, the situation is more straightforward than in *N*-methylformamide. The cis isomer is less accessible, although qualitatively the scheme in Figure 8 remains valid. For the trans-trans *N*-methylacetamide dimer with a single N−H···O=C hydrogen bond, different relative arrangements of the two molecular backbones are conceivable. They have been named α-helical and parallel and antiparallel β-sheet dimers in analogy to the corresponding peptide segments.[88] At the B3LYP/6-311+G* level the antiparallel β-sheet dimer is predicted to be less stable than the α-helical dimer, but the energy difference between the two dimers is less than 1 kJ/mol, so there should not be a strong preference for one of the structures.

Out of the two N−H stretching modes in the dimer, the free one deviates only weakly from the monomer. Therefore, our discussion (see Table 5, last column) concentrates on the hydrogen-bonded N−H fundamental. Depending on the backbone arrangement, a bathochromic shift by 97−114 cm^{-1} relative to the monomer is predicted at the harmonic B3LYP/6-311+G* level. The more stable dimer correlates with the stronger red shift. However, the shift appears to be quite sensitive to the level of calculation, as is the preferred backbone orientation and methyl group conformation. Table 2 in ref 89 contains too many typographical errors to extract a reliable value. Herrebout et al.[16] report 52 cm^{-1} at the B3LYP/6-31G* level, and the structure is closer to that of a parallel β-sheet. Adding a set of diffuse functions more than doubles the shift,[22] and the switch to the PW91 functional increases it further to 171 cm^{-1}. Although these are harmonic values, they underscore the need for a reliable experimental value. In our jet experiment we observe a relatively narrow band with a bathochromic shift of 115 cm^{-1}, which can be assigned to a dimer (see Figure 2, upper trace, and Figure 10). Figure 10 underscores the complementarity of the filet- and popcorn-jet setups. While the room-temperature expansion is dominated by the monomer, the hot expansion contains a higher dimer fraction. The sharpness of the D band may indicate that a single dimer conformation is stabilized in the supersonic expansion. The dimerization shift is in coincidental agreement with the harmonic B3LYP/6-311+G* prediction (see Figure 10), but anharmonic calculations would be desirable.

N-Methylacetamide dimer had been previously assigned in the IR spectrum of diluted CCl_4 solutions.[22] The much smaller red shift by 84 cm^{-1} relative to the monomer is largely due to thermal weakening of the hydrogen bond, but the solvent shift is also substantial. This underscores the importance of jet spectra if reliable benchmark data for quantum treatments of the vibrations are required.

Solution spectra of *N*-methylacetamide also show features due to larger clusters.[89] These may be compared to calculated cluster spectra.[22] For the chain-like trimer, three bands are predicted, the strongest of which is most red shifted (−154 cm^{-1} at the B3LYP/6-31+G* level). A multiparameter deconvolution of the largely unstructured solution band into dimer, trimer, and tetramer contributions allocates this mode 121 cm^{-1} below the monomer. In the jet spectra there is a larger cluster band at 3365 cm^{-1} (see Figure 10), red shifted by 145 cm^{-1} from the monomer band. One may thus tentatively assign this band to a trans *N*-methylacetamide trimer. The second band may be superimposed by the dimer absorption. The enhanced red shift of the lowest N−H stretching mode in the trimer relative to the dimer is due to cooperative effects, which are also reflected in the cluster dissociation energies.[16,22,90]

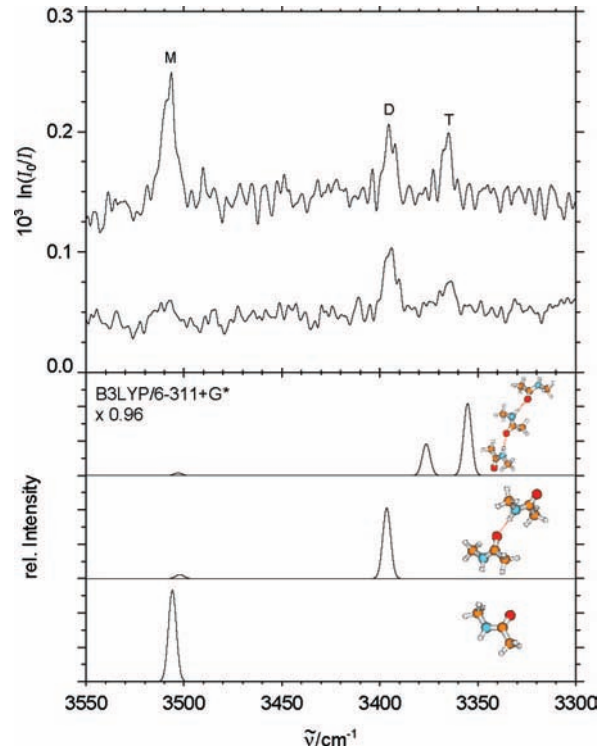

Figure 10. N−H stretching spectra of *N*-methylacetamide in a filet-jet (top, 293 K, 200 coadded spectra) and a popcorn-jet (bottom, 333 K, 600 coadded spectra) expansion, showing the dominant monomer (M), dimer (D), and trimer (T) absorptions in comparison to the calculated wavenumbers for the monomer, dimer, and trimer at the B3LYP/6-311+G* level, scaled by 0.96. Computed intensities are visually matched to experimental peak heights from the filet-jet spectrum and consistent with 3×10^{14} cm^{-3} monomers, 7×10^{12} cm^{-3} dimers, and 3×10^{12} cm^{-3} trimers.

Larger clusters are still predicted to form hydrogen-bonded chains, whereas ring closure analogous to *N*-methylformamide is prevented by methyl group steric hindrance.[89] Their hydrogen-bonded N−H band was observed between 3200 and 3400 cm^{-1} in CCl_4 solution. Liquid *N*-methylacetamide is characterized by even longer hydrogen-bonded linear and branched chains[44] which may shorten with increasing temperature[90] and are structurally related to β-sheet fragments.

N-Methylacetamide was also studied in the carbonyl stretching region (Figure 7), but as in the other investigated amides, an unambiguous assignment is difficult in this region. The monomer band is observed at 1722 cm^{-1}, which is in good agreement with the high-temperature gas-phase data if the average of the P and R branch maxima is taken (see Table 6). Matrix isolation data are systematically shifted to lower wavenumber. The jet result provides a firm benchmark for anharmonic calculations, which have however usually been compared to the matrix data.[29,30] The proper reference reduces the deviation from 42−43 to 27−29 cm^{-1}. The improvement amounts to about one-half of the entire anharmonicity effect in this case.

For the trans-trans *N*-methylacetamide dimer there are two bands expected and predicted by the calculations in the carbonyl region, but the less red-shifted band has a much lower predicted intensity than the second one. Only one dimer band can be clearly observed in the jet spectrum, which is 32 cm^{-1} red shifted to the monomer band. This red shift is somewhat larger than the red shift observed in matrices[6] and the predicted harmonic red shift at the B3LYP level.

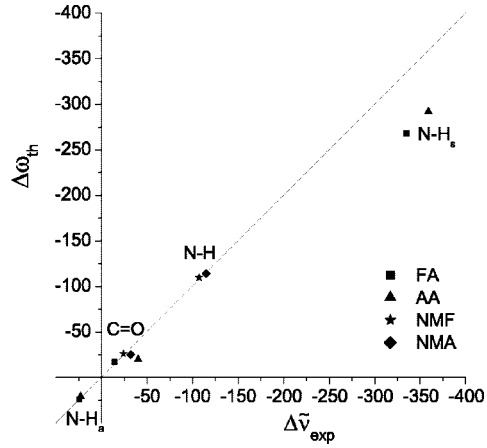

Figure 11. Correlation between experimental anharmonic N−H and C═O stretching fundamental wavenumber shifts $\Delta\tilde{\nu}_{exp}$ and B3LYP/6-311+G* harmonic wavenumber shifts $\Delta\omega_{th}$ relative to the (average) position of the corresponding monomer transitions for all four amides. The diagonal line indicates a perfect correlation.

Huelsekopf et al.[90] provide an approximate correlation between N−H and C═O wavenumbers ($\tilde{\nu}_{C=O}/cm^{-1} = 0.3676\tilde{\nu}_{N-H}/cm^{-1} + 426.1$) which is derived from scaled calculations. Testing this correlation with our observed N−H stretching wavenumber, the equation results in $\tilde{\nu}_{C=O} = 1716\ cm^{-1}$, which differs only by 6 cm^{-1} from the experimentally observed carbonyl stretching vibration and is within the predicted difference of up to 10 cm^{-1} from the measured data.

3.5. Methylation Trends. The harmonic B3LYP calculations performed in this study for comparison purposes reveal some robust trends in the series formamide, acetamide, *N*-methylformamide, and *N*-methylacetamide. C-Methylation lowers the monomer C═O stretching mode by about 30 cm^{-1}, whereas N-methylation lowers it by about 20 cm^{-1}. The experimental C═O stretching fundamentals behave in a qualitatively similar way, but the C-methylation effect is three times smaller. This is also seen in Figure 7, where the scaled monomer prediction is poorer for the monomeric acetamides. Other density functionals behave similarly.[91] Computed N−H stretching fundamentals increase upon C-methylation (at variance with the N−H/C═O correlation [90]) and decrease upon N-methylation, whereas the experimental trends are much weaker.

N-Methylation has a significant influence on the dimer binding energy. The *N*-methylformamide dimer built from two cis units is bound 5 kJ/mol more strongly than the formamide dimer. C-Methylation has a similar effect. This stronger binding persists at higher levels of approximation.[92] It is also reflected in an enhanced bathochromic shift of the N−H vibration upon hydrogen bonding. The experimentally observed difference between the bathochromic shift of the sa band of the formamide dimer and the acetamide dimer (26 cm^{-1}) is well predicted by our calculations at the B3LYP/6-311+G* level (25 cm^{-1}).

Quite generally, harmonic B3LYP/6-311+G* shift predictions correlate well with anharmonic experimental shifts (see Figure 11) with the exception of the acetamide C═O shift and the anharmonic N−H_s stretching modes.

3.6. Ar Matrix Shifts. Table 7 summarizes the matrix shifts experienced by the C═O fundamental and the (symmetric) N−H fundamental of the amides relative to the present jet results. The monomer shifts are bathochromic and range between −8 and −19 cm^{-1}. The dimer shifts, where available, range between +18 and −36 cm^{-1}, even if one concentrates on the most consistent values. This may reflect specific matrix interactions or irregularities in the coupling of the modes. The unusual N−H blue shift for *N*-methylformamide dimer may be related to the various conformations that this singly hydrogen-bonded dimer can adopt. Indeed, annealing promotes more red-shifted dimer absorptions.[25] The surprisingly large formamide dimer N−H red shift in Ar[26] may be related to the weakness of the corresponding matrix band, but it is somewhat unusual that Xe exhibits a smaller red shift. In Figure 4 of ref 26 a more regular Ar band position is quoted (3158.2 cm^{-1}), but that appears to be a typographical error. In any event, the scatter in matrix shifts is of a comparable order of magnitude as anharmonic effects in these amides. In the future, we plan to investigate the Ar matrix shifts more systematically by nanocoating of the jet-expanded monomers and dimers.[9,93]

TABLE 7: Ar Matrix Shifts Relative to the Jet Band Positions of This Work for the C═O Stretching and (Symmetric) N−H Stretching Fundamentals of Amide Monomers (M) and Dimers (D) (in cm^{-1})

C═O	M	D	N−H	M	D
formamide[26]	−15	−12	formamide[26]	−13	−36
acetamide[68]	−18	−12	acetamide[68]	−12	−9
N-methylformamide[25]	−7	∼−3	*N*-methylformamide[25]	−8	+18
N-methylacetamide[6]	−14	−4			

4. Conclusions

This investigation provides for the first time direct absorption vibrational data on hydrogen-bonded dimers of four simple amides in vacuum, which can be directly compared to anharmonic theoretical predictions.[29–31] No matrix, temperature, or solvent shifts have to be considered, and the influence of a range of approximations can be studied reliably. Even harmonic predictions for dimers may be compared to experiment if changes in the anharmonicity constants upon dimerization are neglected. The results allow for a systematic assessment of thermal, matrix embedding, and methylation effects on the vibrational dynamics. They show that non-N-methylated amides form symmetric dimers, whereas singly N-methylated amides conserve their preferred conformation and form singly hydrogen-bonded dimers with separate donor and acceptor roles under the nonequilibrium conditions of a supersonic jet. The results presented here may serve as elementary reference data for IR spectra obtained by impressive UV/IR double-resonance studies on much more complex amides.[33] Furthermore, they should provide a reference for rigorous tests of solvent models, which often suffer from the inseparability of solute and solvent errors.

The study of intermolecular modes[94,95] and combined Raman/IR investigations[16] of amide clusters promise further valuable insights into the dynamics of elementary amide clusters. We are planning such a study using our jet Raman setup[63] after improving its sensitivity for low vapor pressure compounds.

Acknowledgment. The present work was supported by the Fonds der Chemischen Industrie and the DFG research training group 782 (www.pcgg.de). Felix Huff, Alexander Orth, and Jason Park have participated in this work during undergraduate research projects. We thank W. Sander, B. Lucas, and C. Desfrançois for discussions. This work is dedicated to W. Kutzelnigg on the occasion of his 75th birthday. Before pioneering highly accurate electron correlation methods to predict reliable molecular force fields, he measured and analyzed the first acetamide gas-phase spectra in the NH stretching range in the group of R. Mecke.

References and Notes

(1) Guo, H.; Karplus, M. Ab Initio Studies of Hydrogen Bonding of *N*-Methylacetamide: Structure, Cooperativity, and Internal Rotational Barriers. *J. Phys. Chem.* **1992**, *96*, 7273–7287.

(2) Kobko, N.; Dannenberg, J. J. Cooperativity in Amide Hydrogen Bonding Chains. A Comparison between Vibrational Coupling through Hydrogen Bonds and Covalent Bonds. Implications for Peptide Vibrational Spectra. *J. Phys. Chem. A* **2003**, *107*, 6688–6697.

(3) Tan, H.; Qu, W.; Chen, G.; Liu, R. The Role of Charge Transfer in the Hydrogen Bond Cooperative Effect of *cis-N*-Methylformamide Oligomers. *J. Phys. Chem. A* **2005**, *109*, 6303–6308.

(4) Frey, J. A.; Leutwyler, S. An ab Initio Study of Hydrogen Bonded Formamide Dimers. *J. Phys. Chem. A* **2006**, *110*, 12512–12518.

(5) Surewicz, W. K.; Mantsch, H. H.; Chapman, D. Determination of Protein Secondary Structure by Fourier Transform Infrared Spectroscopy: A Critical Assessment. *Biochemistry* **1993**, *32* (2), 389–394.

(6) Torii, H.; Tatsumi, T.; Kanazawa, T.; Tasumi, M. Effects of Intermolecular Hydrogen-Bonding Interactions on the Amide I Mode of N-Methylacetamide: Matrix-Isolation Infrared Studies and ab Initio Molecular Orbital Calculations. *J. Phys. Chem. B* **1998**, *102*, 309–314.

(7) Chalupsky, J.; Vondrášek, J.; Špirko, V. Quasiplanarity of the Peptide Bond. *J. Phys. Chem. A* **2008**, *112*, 693–699.

(8) Dauster, I.; Rice, C. A.; Zielke, P.; Suhm, M. A. N-H$\cdots\pi$ interactions in pyrroles: systematic trends from the vibrational spectroscopy of clusters. *Phys. Chem. Chem. Phys.* **2008**, *10*, 2827–2835.

(9) Rice, C. A.; Borho, N.; Suhm, M. A. Dimerization of Pyrazole in Slit Jet Expansions. *Z. Phys. Chem.* **2005**, *219*, 379–388

(10) Wassermann, T. N.; Rice, C. A.; Suhm, M. A.; Luckhaus, D. Hydrogen bonding lights up overtones in pyrazoles. *J. Chem. Phys.* **2007**, *127*, 234309.

(11) Frey, J. A.; Müller, A.; Losada, M.; Leutwyler, S. Isomers of the Uracil Dimer: An ab Initio Benchmark Study. *J. Phys. Chem. B* **2007**, *111*, 3534–3542.

(12) Gerhards, M.; Unterberg, C.; Gerlach, A.; Jansen, A. β-Sheet model systems in the gas phase: Structures and vibrations of Ac-Phe-NHMe and its dimer (Ac-Phe-NHMe)$_2$. *Phys. Chem. Chem. Phys.* **2004**, *6*, 2682–2690.

(13) Jones, R. L. Infrared Evidence for the Occurrence of Restricted Rotation in N-Methylformamide. *J. Mol. Spectrosc.* **1958**, *2*, 581–586.

(14) Kutzelnigg, W.; Mecke, R. Spektroskopische Untersuchungen an organischen Ionen. 5. Die Struktur der Salze des Acetamids. *Spectrochim. Acta* **1962**, *18*, 549–560.

(15) Florián, J.; Johnson, B. G. Structure, Energetics, and Force Fields of the Cyclic Formamide Dimer: MP2, Hartree-Fock, and Density Functional Study. *J. Phys. Chem.* **1995**, *99*, 5899–5908.

(16) Herrebout, W. A.; Clou, K.; Desseyn, H. O. Vibrational Spectroscopy of N-Methylacetamide Revisited. *J. Phys. Chem. A* **2001**, *105*, 4865–4881.

(17) Kubelka, J.; Keiderling, T. A. Ab Initio Calculation of Amide Carbonyl Stretch Vibrational Frequencies in Solution with Modified Basis Sets. 1. N-Methyl Acetamide. *J. Phys. Chem. A* **2001**, *105*, 10922–10928.

(18) Gómez Marigliano, A. C.; Varetti, E. L. Self-Association of Formamide in Carbon Tetrachloride Solutions: An Experimental and Quantum Chemistry Vibrational and Thermodynamic Study. *J. Phys. Chem. A* **2002**, *106*, 1100–1106.

(19) Cabaleiro-Lago, E. M.; Rodríguez Otero, J. Ab Initio and density functional theory study of the interaction in formamide and thioformamide dimers and trimers. *J. Chem. Phys.* **2002**, *117* (4), 1621–1632.

(20) Watson, T. M.; Hirst, J. D. Density Functional Theory Vibrational Frequencies of Amides and Amide Dimers. *J. Phys. Chem. A* **2002**, *106*, 7858–7867.

(21) Papamokos, G. V.; Demetropoulos, I. N. Vibrational Frequencies of Amides and Amide Dimers: The Assessment of PW91XC Functional. *J. Phys. Chem. A* **2004**, *108*, 7291–7300.

(22) Köddermann, T.; Ludwig, R. N-Methylacetamide/water clusters in a hydrophobic solvent. *Phys. Chem. Chem. Phys.* **2004**, *6*, 1867–1873.

(23) Lucas, B.; Grégoire, G.; Lecomte, F.; Schermann, J.-P.; Desfrançois, C. Infrared spectroscopy of mass-selected neutral molecular systems without chromophore: the formamide monomer and dimer. *Mol. Phys.* **2005**, *103*, 1497–1503.

(24) Lu, J.-f.; Zhou, Z.-y.; Wu, Q.-y.; Zhao, G. Density functional theory study of the hydrogen bonding interaction in formamide dimer. *J. Mol. Struct. (Theochem)* **2005**, *724*, 107–114.

(25) Shin, S.; Kurawaki, A.; Hamada, Y.; Shinya, K.; Ohno, K.; Tohara, A.; Sato, M. Conformational behavior of N-methylformamide in the gas, matrix, and solution states as revealed by IR and NMR spectroscopic measurements and by theoretical calculations. *J. Mol. Struct.* **2006**, *791*, 30–40.

(26) Mardyukov, A.; Sańchez-Garcia, E.; Rodziewicz, P.; Doltsinis, N. L.; Sander, W. Formamide Dimers: A Computational and Matrix Isolation Study. *J. Phys. Chem. A* **2007**, *111*, 10552–10561.

(27) Colominas, C.; Luque, F. J.; Orozco, M. Dimerization of formamide in gas phase and solution. An Ab Initio MC-MST Study. *J. Phys. Chem. A* **1999**, *103*, 6200–6208.

(28) Gaigeot, M. P.; Vuilleumier, R.; Sprik, M.; Borgis, D. Infrared Spectroscopy of N-Methylacetamide Revisited by ab Initio Molecular Dynamics Simulation. *J. Chem. Theory Comput.* **2005**, *1*, 772–789.

(29) Gregurick, S. K.; Chaban, G. M.; Gerber, R. B. Ab Initio and Improved Empirical Potentials for the Calculation of the Anharmonic Vibrational States and Intramolecular Mode Coupling of N-Methylacetamide. *J. Phys. Chem. A* **2002**, *106*, 8696–8707.

(30) Bounouar, M.; Scheurer, C. Reducing the vibrational coupling network in N-methylacetamide as a model for ab initio infrared spectra computations of peptides. *Chem. Phys.* **2006**, *323*, 87–101.

(31) Kaledin, A. L.; Bowman, J. M. Full Dimensional Quantum Calculations of Vibrational Energies of N-Methyl Acetamide. *J. Phys. Chem. A* **2007**, *111*, 5593–5598.

(32) Robertson, E. G.; Hockridge, M. R.; Jelfs, P. D.; Simons, J. P. IR-UV ion-depletion and fluorescence spectroscopy of 2-phenylacetamide clusters: hydration of a primary amide. *Phys. Chem. Chem. Phys.* **2001**, *3*, 786–795.

(33) Shubert, V. A.; Baquero, E. E.; Clarkson, J. R.; James, W. H., III; Turk, J. A.; Hare, A. A.; Worrel, K.; Lipton, M. A.; Schofield, D. P.; Jordan, K. D.; Zwier, T. S. Entropy-driven population distributions in a prototypical molecule with two flexible side chains: O-(2-acetamidoethyl)-N-acetyltyramine. *J. Chem. Phys.* **2007**, *127*, 234315.

(34) Borba, A.; Gómez-Zavaglia, A.; Fausto, R. Molecular Structure, Vibrational Spectra, Quantum Chemical Calculations and Photochemistry of Picolinamide and Isonicotinamide Isolated in Cryogenic Inert Matrixes and in the Neat Low-Temperature Solid Phases. *J. Phys. Chem. A* **2008**, *112*, 45–57.

(35) Pohl, G.; Perczel, A.; Vass, E.; Magyarfalvi, G.; Tarczay, G. A matrix isolation study on Ac-Gly-NHMe and Ac-L-Ala-NHMe, the simplest chiral and achiral building blocks of peptides and proteins. *Phys. Chem. Chem. Phys.* **2007**, *9*, 4698–4708.

(36) Demaison, J.; Császár, A. G.; Kleiner, I.; Møllendal, H. Equilibrium vs ground-state planarity of the CONH linkage. *J. Phys. Chem. A* **2007**, *111*, 2574–2586.

(37) McNaughton, D.; Evans, C. J.; Lane, S.; Nielsen, C. J. The High-Resolution FTIR Far-Infrared Spectrum of Formamide. *J. Mol. Spectrosc.* **1999**, *193*, 104–117.

(38) Jurečka, P.; Sponer, J.; Černý, J.; Hobza, P. Benchmark database of accurate (MP2 and CCSD(T) complete basis set limit) interaction energies of small model complexes, DNA base pairs, and amino acid pairs. *Phys. Chem. Chem. Phys.* **2006**, *8*, 1985–1993.

(39) Schwabe, T.; Grimme, S. Double-hybrid density functionals with long- range dispersion corrections: higher accuracy and extended applicability. *Phys. Chem. Chem. Phys.* **2007**, *9*, 3397–3406.

(40) Fantoni, A. C.; Caminati, W.; Hartwig, H.; Stahl, W. The very low methyl group V_3 barrier of cis N-methylformamide: A-E doubling from the free jet rotational spectrum. *J. Mol. Spectrosc.* **2002**, *612*, 305–307.

(41) Fantoni, A. C.; Caminati, W. Rotational spectrum and ab initio calculations of N-methylformamide. *J. Chem. Soc., Faraday Trans.* **1996**, *92* (3), 343–346.

(42) Wiberg, K. B.; Rush, D. J. Methyl Rotational Barriers in Amides and Thioamides. *J. Org. Chem.* **2002**, *67*, 826–830.

(43) Avalos, M.; Babiano, R.; Barneto, J. L.; Bravo, J. L.; Cintas, P.; Jiménez, J. L.; Palacios, J. C. Can we predict the conformational preference of amides? *J. Org. Chem.* **2001**, *66*, 7275–7282.

(44) Whitfield, T. W.; Martyna, G. J.; Allison, S.; Bates, S. P.; Vass, H.; Crain, J. Structure and Hydrogen Bonding in Neat N-Methylacetamide: Classical Molecular Dynamics and Raman Spectroscopy Studies of a Liquid of Peptidic Fragments. *J. Phys. Chem. B* **2006**, *110*, 3624–3637.

(45) Nesbitt, D. J. High-resolution, direct infrared laser absorption spectroscopy in slit supersonic jets: intermolecular forces and unimolecular vibrational dynamics in clusters. *Annu. Rev. Phys. Chem.* **1994**, *45*, 367–399.

(46) Liu, K.; Fellers, R. S.; Viant, M. R.; McLaughlin, R. P.; Brown, M. G.; Saykally, R. J. A long path length pulsed slit valve appropriate for high temperature operation: Infrared spectroscopy of jet-cooled large water clusters and nucleotide bases. *Rev. Sci. Instrum.* **1996**, *67*, 410–416.

(47) Borho, N.; Suhm, M. A.; Le Barbu-Debus, K.; Zehnacker, A. Intra- vs. Intermolecular Hydrogen Bonding: Dimers of alpha-Hydroxyesters with Methanol. *Phys. Chem. Chem. Phys.* **2006**, *8*, 4449–4460.

(48) In a continuation of our culinary acronyms for different nozzle and cluster spectrometer designs, we denote this nozzle as *pop*pet *co*ntrolled *r*esistively heated *n*ozzle (popcorn) having in mind the liquid-soaked molecular sieve or crystal grains which deliver the required vapor pressure upon heating.

(49) Cézard, C.; Rice, C. A.; Suhm, M. A. OH-Stretching Redshifts in Bulky Hydrogen-Bonded Alcohols: Jet Spectroscopy and Modeling. *J. Phys. Chem. A* **2006**, *110*, 9839–9848.

(50) Fárník, M.; Weimann, M.; Suhm, M. A. Acidic protons before take-off: A comparative jet Fourier transform infrared study of small HCl- and HBr-solvent complexes. *J. Chem. Phys.* **2003**, *118*, 10120–10136.

(51) Frisch, M. J.; Trucks, G. W.; Schlegel, H. B.; Scuseria, G. E.; Robb, M. A.; Cheeseman, J. R.; Montgomery, J. A., Jr.; Vreven, T.; Kudin, K. N.; Burant, J. C.; Millam, J. M.; Iyengar, S. S.; Tomasi, J.; Barone, V.; Mennucci, B.; Cossi, M.; Scalmani, G.; Rega, N.; Petersson, G. A.; Nakatsuji, H.; Hada, M.; Ehara, M.; Toyota, K.; Fukuda, R.; Hasegawa, J.; Ishida, M.; Nakajima, T.; Honda, Y.; Kitao, O.; Nakai, H.; Klene, M.; Li, X.; Knox, J. E.; Hratchian, H. P.; Cross, J. B.; Adamo, C.; Jaramillo, J.; Gomperts, R.; Stratmann, R. E.; Yazyev, O.; Austin, A. J.; Cammi, R.; Pomelli, C.; Ochterski, J. W.; Ayala, P. Y.; Morokuma, K.; Voth, G. A.; Salvador, P.; Dannenberg, J. J.; Zakrzewski, V. G.; Dapprich, S.; Daniels, A. D.; Strain, M. C.; Farkas, O.; Malick, D. K.; Rabuck, A. D.; Raghavachari, K.; Foresman, J. B.; Ortiz, J. V.; Cui, Q.; Baboul, A. G.; Clifford, S.; Cioslowski, J.; Stefanov, B. B.; Liu, G.; Liashenko, A.; Piskorz, P.; Komaromi, I.; Martin, R. L.; Fox, D. J.; Keith, T.; Al-Laham, M. A.; Peng, C. Y.; Nanayakkara, A.; Challacombe, M.; Gill, P. M. W.; Johnson, B.; Chen, W.; Wong, M. W.; Gonzalez, C.; Pople, J. A. *Gaussian 03, Revisions B. 04 and C. 02*; Gaussian Inc.: Pittsburgh, PA, 2003.

(52) Wong, M. W.; Wiberg, K. B. Structure of Acetamide: Planar or Nonplanar. *J. Phys. Chem.* **1992**, *96*, 668–671.

(53) Samdal, S. Acetamide, a challenge to theory and experiment? On the molecular structure, conformation, potential to internal rotation of the methyl group and force fields of free acetamide as studied by quantum chemical calculations. *J. Mol. Struct.* **1998**, *440*, 165–174.

(54) Jeffrey, G. A.; Ruble, J. R.; McMullan, R. K.; DeFrees, D. J.; Binkley, J. S.; Pople, J. A. Neutron Diffraction at 23 K and ab initio Molecular-Orbital Studies of the Molecular Structure of Acetamide. *Acta Crystallogr,, Sect. B* **1980**, *36*, 2292–2299.

(55) Brummel, C. L.; Shen, M.; Hewett, K. B.; Philips, L. A. High-resolution infrared spectroscopy of formamide and deuterated formamide in a molecular beam. *J. Opt. Soc. Am. B.* **1994**, *11* (1), 176–183.

(56) Zhao, Y.; Truhlar, D. G. Infinite-Basis Calculations of Binding Energies for the Hydrogen Bonded and Stacked Tetramers of Formic Acid and Formamide and Their Use for Validation of Hybrid DFT and ab Initio Methods. *J. Phys. Chem. A* **2005**, *109* (30), 6624–6627.

(57) Ladell, J.; Post, B. The Crystal Structure of Formamide. *Acta Crystallogr.* **1954**, *7*, 559–564.

(58) Iogansen, A. V.; Kurkchi, G. A.; Dementjeva, L. A. Infrared spectra in the ν_{NH} region and structures of associated species of acetamide. *J. Mol. Struct.* **1976**, *35*, 101–114.

(59) Räsänen, M. A Matrix Infrared Study of Monomeric Formamide. *J. Mol. Struct.* **1983**, *101*, 275–286.

(60) Räsänen, M. A Matrix Infrared Study of Association of Formamide. *J. Mol. Struct.* **1983**, *102*, 235–242.

(61) King, S. T. Infrared Study of the NH_2 "Inversion" Vibration for Formamide in the Vapor Phase and in an Argon Matrix. *J. Phys. Chem.* **1971**, *75* (3), 405–410.

(62) Larsen, R. W.; Zielke, P.; Suhm, M. A. Hydrogen-bonded OH stretching modes of methanol clusters: A combined IR and Raman isotopomer study. *J. Chem. Phys.* **2007**, *126*, 194307.

(63) Zielke, P.; Suhm, M. A. Concerted proton motion in hydrogen-bonded trimers: A spontaneous Raman scattering perspective. *Phys. Chem. Chem. Phys.* **2006**, *8*, 2826–2830.

(64) Rice, C. A.; Dauster, I.; Suhm, M. A. Infrared spectroscopy of pyrrole-2-carboxaldehyde and its dimer: A planar β-sheet peptide model? *J. Chem. Phys.* **2007**, *126*, 134313.

(65) Emmeluth, C.; Suhm, M. A.; Luckhaus, D. A monomers-in-dimers model for carboxylic acid dimers. *J. Chem. Phys.* **2003**, *118*, 2242–2255.

(66) Duvernay, F.; Chatron-Michaud, P.; Borget, F.; Birney, D. M.; Chiavassa, T. Photochemical dehydration of acetamide in a cryogenic matrix. *Phys. Chem. Chem. Phys.* **2007**, *9*, 1099–1106.

(67) Knudsen, R.; Sala, O.; Hase, Y. A low temperature matrix isolation infrared study of acetamides. I. Acetamide and some deuterated derivatives. *J. Mol. Struct.* **1994**, *321*, 187–195.

(68) King, S. T. Low temperature matrix isolation study of hydrogen-bonded, high-boiling organic compounds-III Infrared spectra of monomeric acetamide, urea and urea-d_4. *Spectrochim. Acta, Part A* **1972**, *28*, 165–175.

(69) Emmeluth, C.; Suhm, M. A. A chemical approach towards the spectroscopy of carboxylic acid dimer isomerism. *Phys. Chem. Chem. Phys.* **2003**, *5*, 3094–3099.

(70) Davies, M.; Hallam, H. E., III. Molecular interaction and infrared absorption spectra. Part III. Acetamide *Trans. Faraday Soc.* **1951**, *47* (11), 1170–1181.

(71) Denne, W. A.; Small, R. W. H. A refinement of the structure of rhombohedral acetamide. *Acta Crystallogr., Sect. B* **1971**, *27*, 1094–1098.

(72) Senti, F.; Harker, D. The Crystal Structure of Rhombohedral Acetamide. *J. Am. Chem. Soc.* **1940**, *62*, 2008–2019.

(73) NIST Chemistry WebBook: http://webbook.nist.gov/chemistry.

(74) Ataka, S.; Takeuchi, H.; Tasumi, M. Infrared studies of the less stable cis form of N-Methylformamide and N-Methylacetamide in low-temperature nitrogen matrices and vibrational analyses of the trans and cis forms of these molecules. *J. Mol. Struct.* **1984**, *113*, 147–160.

(75) Miyazawa, T. Normal Vibrations of Monosubstituted Amides in the cis Configuration and Infrared Spectra of Diketopiperazine. *J. Mol. Spectrosc.* **1960**, *4*, 155–167.

(76) Hallam, H. E.; Jones, C. M. Molecular Configuration and Interactions of the Amide Group. *Trans. Faraday Soc.* **1969**, *65*, 2607–2610.

(77) Kitano, M.; Kuchitsu, K. Molecular Structure of N-Methylformamide as Studied by Gas Electron Diffraction. *Bull. Chem. Soc. Jpn.* **1974**, *47*, 631–634.

(78) Jones, R. L. The Infrared Spectra of Some Simple N-Substituted Amides in the Vapor State. *J. Mol. Spectrosc.* **1963**, *11*, 411–421.

(79) Nandini, G.; Sathyanarayana, D. N. Ab initio studies on geometry and vibrational spectra of N-methylformamide and N-methylacetamide. *J. Mol. Struct. (Theochem)* **2002**, *579*, 1–9.

(80) Martínez, A. G.; Vilar, E. T.; Fraile, A. G.; Martínez-Ruiz, P. A Computational and Experimental Study on the Relative Stabilities of Cis and Trans Isomers of N-Alkylamides in Gas Phase and in Solution. *J. Phys. Chem. A* **2002**, *106*, 4942–4950.

(81) Scheurer, C.; Piryatinski, A.; Mukamel, S. Signatures of β-peptide unfolding in two-dimensional vibrational echo spectroscopy: A simulation study. *J. Am. Chem. Soc.* **2001**, *123*, 3114–3124.

(82) Martínez, A. G.; Vilar, E. T.; Fraile, A. G.; Martínez-Ruiz, P. Density functional theory study of self-association of N-methylformamide and its effect on intramolecular and intermolecular geometrical parameters and the cis/trans population. *J. Chem. Phys.* **2006**, *124*, 324305.

(83) LaPlanche, L. A.; Rogers, M. T. cis and trans Configuration of the Peptide Bond in N-Monosubstituted Amides by Nuclear Magnetic Resonance. *J. Am. Chem. Soc.* **1964**, *86* (3), 337–341.

(84) Ludwig, R.; Weinhold, F.; Farrar, T. C. Theoretical Study of hydrogen bonding in liquid and gaseous N-methylformamide. *J. Chem. Phys.* **1997**, *107* (2), 499–507.

(85) Woutersen, S.; Mu, Y.; Stock, G.; Hamm, P. Hydrogen-bond lifetime measured by time-resolved 2D-IR spectroscopy: N-methylacetamide in methanol. *Chem. Phys.* **2001**, *266*, 137–147.

(86) Jorgensen, W. L.; Gao, J. Cis-Trans Energy Difference for the Peptide Bond in the Gas Phase and in Aqueous Solution. *J. Am. Chem. Soc.* **1988**, *110*, 4212–4216.

(87) Bednárová, L.; Malon, P.; Bour, P. Spectroscopic Properties of the Nonpolar Amide Group: A Computational Study. *Chirality* **2007**, *19*, 775–786.

(88) Ham, S.; Cho, M. Amide I modes in the N-methylacetamide dimer and glycine dipeptide analog: Diagonal force constants. *J. Chem. Phys.* **2003**, *118* (15), 6915–6922.

(89) Ludwig, R.; Reis, O.; Winter, R.; Weinhold, F.; Farrar, T. C. Quantum Cluster Equilibrium Theory of Liquids: Temperature Dependence of Hydrogen Bonding in Liquid N-Methylacetamide Studied by IR Spectra. *J. Phys. Chem. B* **1998**, *102*, 9312–9318.

(90) Huelsekopf, M.; Ludwig, R. Correlations between structural, NMR and IR spectroscopic properties of N-methylacetamide. *Magn. Reson. Chem.* **2001**, *39*, S127–S134.

(91) Watson, T. M.; Hirst, J. D. Calculating vibrational frequencies of amides: From formamide to concanavalin A. *Phys. Chem. Chem. Phys.* **2004**, *6*, 998–1005.

(92) Langley, C. H.; Allinger, N. L. Molecular Mechanics (MM4) and ab Initio Study of Amide-Amide and Amide-Water Dimers. *J. Phys. Chem. A* **2003**, *107*, 5208–5216.

(93) Wassermann, T. N.; Zielke, P.; Lee, J. J.; Cézard, C.; Suhm, M. A. Structural preferences, argon nanocoating, and dimerization of n-alkanols as revealed by OH stretching spectroscopy in supersonic jets. *J. Phys. Chem. A* **2007**, *111*, 7437–7448.

(94) Tam, C. N.; Bour, P.; Eckert, J.; Trouw, F. R. Inelastic Neutron Scattering Study of Hydrogen-Bonded Solid Formamide at 15 K. *J. Phys. Chem. A* **1997**, *101*, 5877–5884.

(95) Torii, H.; Tasumi, M. Intermolecular Hydrogen Bonding and Low-Wave-Number Vibrational Spectra of Formamide, N-Methylformamide, and N-Methylacetamide in the Liquid State. *Int. J. Quantum Chem.* **1998**, *70*, 241–252.

(96) Engdahl, A.; Nelander, B.; Astrand, P.-O. Complex formation between water and formamide. *J. Chem. Phys.* **1993**, *99*, 4894–4907.

(97) Miyazawa, T.; Shimanouchi, T.; Mizushima, S-I. Characteristic Infrared Bands of Monosubstituted Amides. *J. Chem. Phys.* **1956**, *24* (2), 408–418.

JP8039912